Chemical Physics 163 (1992) 193–208
North-Holland

# Acetone, a laser-induced fluorescence study with rotational resolution at 320 nm

Hanna Zuckermann, Yehuda Haas
*Department of Physical Chemistry and The Farkas Center for Light Induced Processes, The Hebrew University, Jerusalem 91904, Israel*

Marcel Drabbels, Johannes Heinze, W. Leo Meerts, Joerg Reuss
*Molecular and Laser Physics, University of Nijmegen, Toernooiveld, 6525 ED Nijmegen, The Netherlands*

and

John van Bladel
*Department of Theoretical Chemistry, University of Nijmegen, Toernooiveld, 6525 ED Nijmegen, The Netherlands*

Received 1 March 1992

The forbidden $S_1 \leftarrow S_0$ transition of acetone has been investigated by laser-induced fluorescence measurements with a resolution of 270 MHz. The rotational structure demonstrates, that (i) one deals with a-type transitions and (ii) there is a strong coupling between the torsional motion of the two $CH_3$ groups and the tunneling, out-of-plane wagging motion ($\nu_{23}$) of acetone. The interpretation of torsion–vibrational combination bands is less conclusive and thus the discussion still has a preliminary character.

## 1. Introduction

Formaldehyde ($H_2CO$) exhibits a lowest energy $^1n\pi^*$ transition that is strictly forbidden in $C_{2v}$ and is extremely weak, $f \approx 10^{-3}$. The observed intensity is vibronically induced. The C=O out-of-plane wagging motion ($\nu_4$) is the $b_1$ vibration that makes the $A_2 \leftarrow A_1$ transition allowed, via intensity borrowing from the $B_2(n,\sigma^*)$ higher lying state [1,2]. Proof of this mechanism was provided by the observation of a-type rovibronic structure in the high resolution electronic spectrum of $H_2CO$ [3].

A similar mechanism was expected to apply to acetone, $(CH_3)_2CO$, where $A_2 \leftarrow A_1$ transition is also very weak, $f \approx 4 \times 10^{-4}$ [4]. But Baba, Hanazaki and Nagashima (BHN) [5], and Zuckermann et al. [6,7], in studies of the low resolution fluorescence excitation spectrum of acetone, concluded that many of the bands are c-type. Therefore, it appeared that the vibronic coupling mechanism responsible for the observed intensity in the $S_1 \leftarrow S_0$ transition of acetone is different from that in formaldehyde.

The previous experiments on acetone were performed at a resolution of 0.2 $cm^{-1}$. Now, contour analysis of weak transitions is potentially subject to errors owing to fluctuations in laser intensity and to mode hopping within the 0.2 $cm^{-1}$ bandwidth. For this reason, we have re-examined the $S_1 \leftarrow S_0$ spectrum of acetone at high resolution, 0.01 $cm^{-1}$. We find that the low lying bands are all pure a-type, a result that is consistent with the earlier results on formaldehyde. Additionally, for the lowest vibrational $S_1$ level we find a constant threefold splitting of each rotational line. (More complex splitting patterns are observed in higher energy bands.) We show in this paper that these splittings have their origin in the methyl group torsional motion.

In addition to the torsional motion we concern ourselves here also with other low frequency vibrations of acetone, in the $S_1$ state. Table 1 summarizes the available data on the five lowest frequency ground

Table 1
Low frequency vibrational modes of acetone in the ground electronic state

| Symm. species ($C_{2v}$) | No. | Description | Frequency ($cm^{-1}$) | Ref. | Comments |
|---|---|---|---|---|---|
| $a_2$ | $\nu_{12}$ | "antigearing" torsion | 77 | [8] | |
| $b_1$ | $\nu_{24}$ | "gearing" torsion | 124 | [9] | |
| $a_1$ | $\nu_8$ | C-C-C bending | 385 | [10,11] | ref. [12] reversed the assignment of $\nu_8$ and $\nu_{23}$ but ref. [13] reconfirms it |
| $b_1$ | $\nu_{23}$ | C=O out-of-plane wagging | 484 | [12] | in ref. [12] this is $b_2$ |
| $b_2$ | $\nu_{19}$ | C=O in-plane wagging | 530 | [11] | in ref. [12] this is $b_1$ |

state modes. The inertial axes and the torsional angles are shown in fig. 1. The two torsional fundamentals have been assigned only recently, and fitted to a hindered two rotor potential [14]. The assignment of the 385 $cm^{-1}$ vibration to the C-C-C bend and the 484 $cm^{-1}$ vibration to the C=O out-of-plane wagging motion has been controversial [10–13].

The ground state torsional potential has been calculated by several authors [15–18] in an attempt to account for the microwave spectrum. The $\nu_{12}$ vibration, which is infrared inactive and very weakly Raman active, has been observed by two-photon jet spectroscopy involving Rydberg transitions [8], leading to a revised calculation [14], in which complete geometry optimization for each conformer was allowed. This calculation, using only four terms in the torsional potential ($V_3$, $V_{33}$, $V'_{33}$, and $V_6$) led to good agreement with the experimental results, and to an effective torsional barrier ($V_{eff}=V_3-V_{33}$) of 240 $cm^{-1}$, somewhat lower than previously determined barrier [15,16] of 270 $cm^{-1}$.

In the $A_2(n\pi^*)$ state the $\nu_{23}$ vibration is described by a double well potential and thus subject to tunnel splitting, in contrast to the ground state case. A complete analysis of the spectrum thus involves two multiple-well potentials that may lead to tunnel splitting: that of the torsion ($3^2$-fold) and of the C=O out-of-plane wagging motion (2-fold). It turns out that some interaction between these two modes is required to account for the rotational fine structure in certain bands. In all bands, the $\nu_{23}$ mode is involved via at least one of its tunnel split levels.

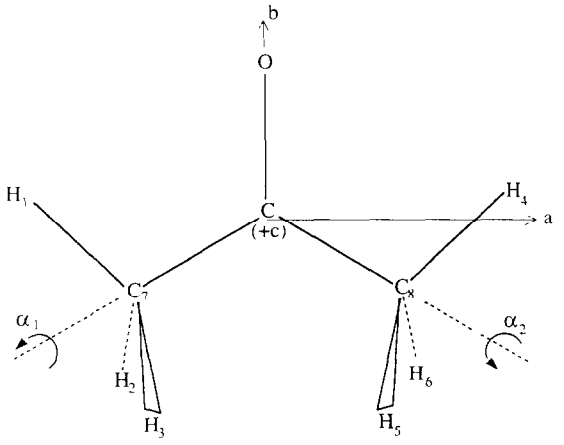


Fig. 1. Schematic presentation of the structure of acetone.

## 2. Experimental

Narrow bandwidth radiation with a high peak power is obtained by pulsed amplification of radiation from a cw ring dye laser. The ring dye laser (Spectra Physics, 380D) is pumped by 6 W of an argon ion laser (Spectra Physics, 2045-15) and operates on DCM dye (620–660 nm). The bandwidth of the ring dye laser is less than 0.5 MHz and the output power is typically 400 mW. This radiation is amplified by a home-built four-stage pulsed dye amplifier (PDA) system similar to the system described by Cromwell et al. [19]. A frequency doubled *Q*-switched Nd:YAG laser (Quantel YG 681C-10) with a pulse length of 5 ns and a pulse energy of 550 mJ pumps the PDA system. The pulse energy of the amplified laser beam is 100 mJ. The bandwidth, which is merely determined by the Fourier limit of the pulsed pumped laser is measured with a 300 MHz

Fabry–Perot interferometer and amounts to 135 MHz. This light is then frequency doubled in a KDP crystal. The UV beam (310–330 nm) is separated from the fundamental beam by a Pellin Broca prism. The pulse energy of the UV light is 20 mJ. For absolute frequency calibration the iodine absorption spectrum [20] is recorded. For relative frequency calibration the transmission fringes of a temperature stabilized Fabry–Perot interferometer with a free spectral range of 598.82 MHz are recorded.

A molecular beam of acetone is formed by expanding a 5% mixture of acetone in argon through a modified electromagnetic fuel injector valve (Bosch) with an orifice diameter of 1 mm into a vacuum chamber. During operation the background pressure in the vacuum chamber is $5\times10^{-5}$ Torr. The commercially obtained acetone (Merck 99.5%) is used without further purification. The stagnation pressure used during the experiments is 2 atm.

The laser beam with a diameter of 3 mm crosses the molecular beam 45 mm downstream the nozzle. The laser induced fluorescence is collected by a quartz lens system and imaged onto the photocathode of a photomultiplier (EMI 9863B). To reduce the scattered laser light a Schott KV 370 glass filter is placed in front of the photomultiplier. The fluorescence signal is processed by a digital oscilloscope (LeCroy 7400) and a boxcar integrator (SRS 250) interfaced with a PDP 11/23 computer.

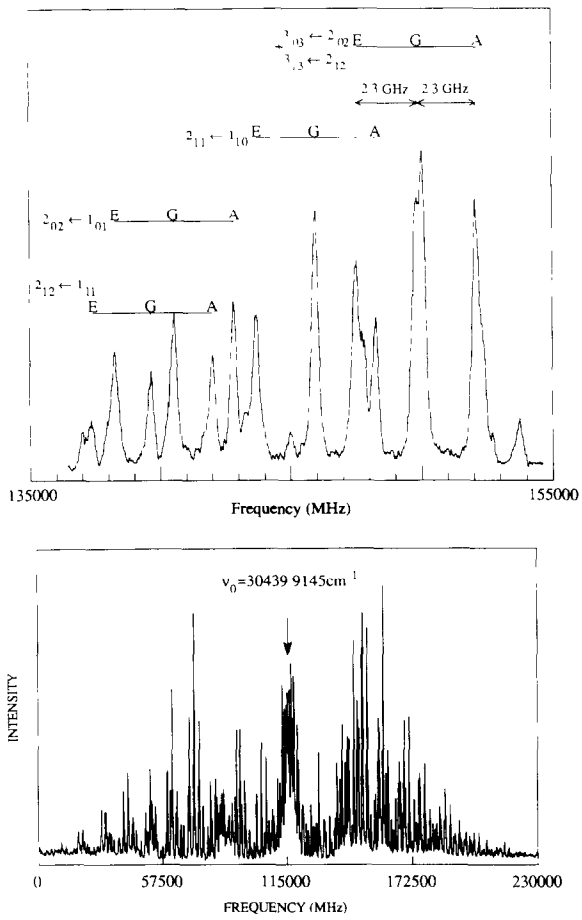


Fig. 2. Lower panel: the high resolution spectrum of line 1, the band origin indicated in the figure is calculated for the transitions of G-symmetry, of which some are shown in the upper panel. Upper panel: measured splittings (in GHz) and proposed assignments of the fine structure. The splittings, shown for some multiplets only, hold for the entire spectrum.

## 3. Spectroscopic results and analysis

We have studied at high resolution the first 14 bands reported by BHN. figs. 2–4 show the fluorescence excitation spectra of some bands with their tunnel splitting fine structure. Those are the bands where a satisfactory fit to an asymmetric rotor Hamiltonian could be obtained. In table 2 we summarize the main features of the bands, using BHN's line numbering system. Three main conclusions may be drawn from the results:

(i) All transitions are a-type, namely polarized in the molecular plane, perpendicular to the C=O bond. (In $C_{2v}$, this polarization belongs to the $B_2$ irreducible representation.)

(ii) The largest change of the inertial moment on excitation to $S_1$ is with respect to the *b* axis, i.e. along the C=O bond, as expressed by the relatively large change in the *B* rotational constant. This is indeed expected if the excited state is non-planar, as in formaldehyde, with the central carbon atom becoming the apex of a pyramid whose base is formed by the two other carbon atoms and the oxygen atom.

(iii) Each of the rotational lines is split into a multiplet.

### *3.1. Analysis of the $0_0^0$ band*

The lowest frequency transition observed (line 1, table 2) was assigned by BHN as the $0_0^0$ band. We

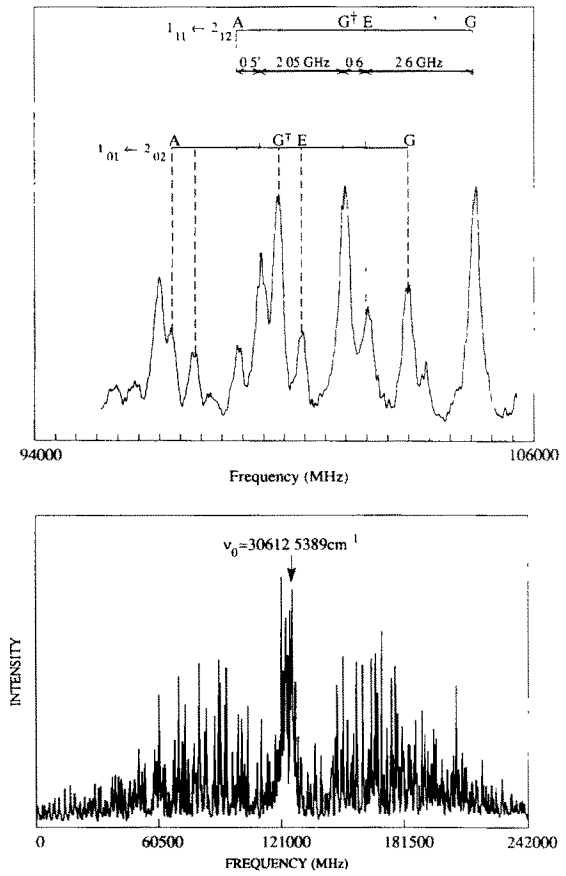


Fig. 3. As in fig. 2, for line 2. The G†-transitions served to determine the band origin.

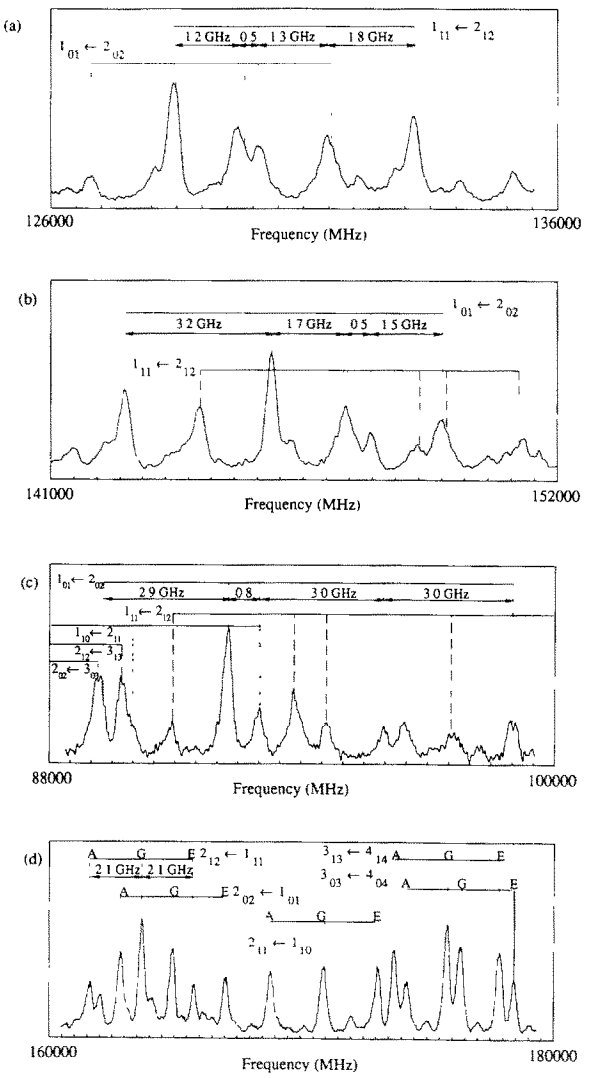


Fig. 4. (a) As in fig. 2, upper panel, for line 4. The symmetry species of the quintets have not been assigned. (b) As in fig. 2, upper panel, for line 5. The symmetry species of the quintets have not been assigned. (c) As in fig. 2, upper panel, for line 6. The symmetry species of the quintets have not been assigned. (d) As in fig. 2, upper panel, for line 7. A triplet structure has been found.

have studied it with a resolution of 270 MHz, and fig. 2 shows the fluorescence excitation spectrum. Table 3 lists the observed transitions and their assignments. Within the experimental error of 50 MHz every observed rotational line in the spectrum could be fit to the asymmetric rotor Hamiltonian. The observed triplet splitting remains constant for all rotational quantum numbers and amounts to 2.3 GHz. This splitting arises from either (or both) tunnel splittings expected in this system: the one due to the three-fold potential of the $CH_3$ torsional motion, and the one due to the double well potential of the C=O out-of-plane wagging. The first is expected to be present in both $S_0$ and $S_1$, and the latter only in $S_1$.

Since the transition is pure a-type, we can determine the symmetry species of the excited state. We shall begin by assuming that the system can be discussed within the $C_{2v}$ point group as far as the $n\pi^*$ transition is concerned. The main justification for this assumption is the fact that the $S_1 \leftarrow S_0$ oscillator strength in acetone is very small, similar to that of formaldehyde. The physical reason is that in $S_0$ the local symmetry of the C=O bond is close enough to

Table 2
Main experimental results for the vibronic bands

| Line [a] | Frequency [b] ($cm^{-1}$) | Type [c] | Rotational constants [d] (MHz) | | | Fine structure |
|---|---|---|---|---|---|---|
| | | | $\Delta A$ | $\Delta B$ | $\Delta C$ | |
| 1 | 0 | a | 60.2(7.1) | −341.9(3.4) | −14.4(1.1) | triplet |
| 2 | 172.6244 | a | 78.8(5.7) | −351.5(2.8) | 10.9(0.6) | quintet |
| 3 | not observed hot band | | | | | |
| 4 | 314.5463 | a | 68.1(7.5) | −362.9(2.7) | −29.7(1.2) | quintet |
| 5 | 333.5593 | a | 87.4(6.2) | −371.3(3.0) | −32.0(0.3) | quintet |
| 6 | 346.3927 | a | 23.8(8.9) | −381.9(5.2) | −23.8(1.2) | quintet |
| 7 | 373 | a | | | | triplet |
| 8 | 473.4 | a | | | | > quintet [e] |
| | 474.4 | a | | | | |
| 9 | 486.7 | a | | | | quintet [e,f] |
| 10 | 509.7275 | a | 42.4(6.1) | −437.4(16) | −23.9(1.8) | |
| | 510.1171 | a | 139.97(9.8) | −525.4(6.7) | −20.5(1.3) | [e] |
| | 510.3715 | a | 53.44(8.0) | −408.9(6.9) | −37.1(0.6) | |
| 11 | 544 | | | | | |
| 12 | 578 | | | | | |
| 13a | 621.76 | a | 107.8(11) | −303.7(7.2) | −40.9(0.6) | |
| 13b | 624 | | | | | quintet [e,g] |
| 14 | 645 | | | | | |

[a] The numbering system is the same as used by BHN (ref. [1]).
[b] Frequencies above the $0_0^0$ transition, $\nu_0 = 30439.9145\ cm^{-1}$; $\nu_0$ was used in calculation for fitted lines only; other frequencies are estimated centers of bands.
[c] Using the axis convention of scheme I.
[d] Listed are the changes in the three principal rotational constants with respect to the ground state constants, which are (MHz): $A = 10165.6$, $B = 8514.9$, $C = 4910.2$. The standard deviation of the fit is given in the parentheses.
[e] Analysis in progress.
[f] Five components are observed with approximate relative shifts of 20, 9, 13 and 9 GHz.
[g] Five components are observed with approximate relative shifts of 16, 8, 4 and 9 GHz.

$C_{2v}$, so that $C_{2v}$ selection rules hold almost rigorously. Furthermore, the fact that the two pyramidal forms of $S_1$ are interconverting by tunneling motion, means that $C_{2v}$ should be used rather than $C_S$. As we shall see, predictions based on those rules agree well with experimental observations.

In the jet experiments, all transitions are assumed to originate from the vibrational ground state, which is $A_1$. The $n\pi^*$ electronic state transforms as $A_2$. We write the transition dipole moment as

$$\mu_{fi} = \langle \Psi'_{ev} | \hat{\mu} | \Psi''_{ev} \rangle , \qquad (1)$$

where $\Psi'_{ev}$ and $\Psi''_{ev}$ are vibronic wavefunctions of the upper and lower vibronic states, respectively, and require that $\mu_{fi}$ is of $A_1$ symmetry. The direct product of the irreducible representations (irreps) of the terms appearing in (1) is

$$A_1 = \Gamma(\Psi'_e) \otimes \Gamma(\hat{\mu}) \otimes \Gamma(\Psi''_e) \otimes \Gamma(X'_v) \otimes \Gamma(X''_v)$$
$$= A_2 \otimes B_2 \otimes A_1 \otimes \Gamma(X'_v) \otimes A_1 = B_1 \otimes \Gamma(X'_v) \qquad (2)$$

($A_3 \otimes A_4 \otimes A_1 \otimes \Gamma(X'_v) \otimes A_1 = A_2 \otimes \Gamma(X'_v)$ in $G_{36}$, see below) meaning that the vibrational wavefunction of $S_1$ must transform as $B_1$ in order to make the transition allowed; the real zero point vibrational wavefunction is totally symmetric ($A_1$). A transition to this lowest state is therefore forbidden. The first observed transition will be to a low vibrational level of $B_1$ symmetry, which e.g. might arise from tunnel splitting of one of the multiple well motions.

We start the theoretical analysis of the torsional vibrations with the assumption that interactions between torsion vibrations and other normal vibrations of the molecule can be neglected. In this case, it is

Table 3
Observed and calculated rovibronic frequencies of the $S_1 \leftarrow S_0 0_0^0$ vibronic transition relative to the center frequency $\nu_0 = 30439.9145$ $cm^{-1}$

| Calculated frequency (MHz) | Observed frequency (MHz) | Obs. − calc. (MHz) | $J''$ | $K''_{-1}$ | $K''_1$ | $J'$ | $K'_{-1}$ | $K'_1$ |
|---|---|---|---|---|---|---|---|---|
| −54556 | −54557 | − 1 | 5 | 0 | 5 | 4 | 0 | 4 |
| −54527 | −54557 | −30 | 5 | 1 | 5 | 4 | 1 | 4 |
| −55421 | −55461 | −40 | 4 | 1 | 3 | 3 | 1 | 2 |
| −52852 | −52881 | −29 | 4 | 2 | 3 | 3 | 2 | 2 |
| −47180 | −47219 | −39 | 3 | 2 | 1 | 2 | 2 | 0 |
| −44525 | −44462 | 63 | 3 | 1 | 2 | 2 | 1 | 1 |
| −40435 | −40426 | 9 | 3 | 2 | 2 | 2 | 2 | 1 |
| −34645 | −34616 | 29 | 3 | 0 | 3 | 2 | 0 | 2 |
| −34021 | −33957 | 64 | 3 | 1 | 3 | 2 | 1 | 2 |
| −30768 | −30709 | 59 | 2 | 1 | 1 | 1 | 1 | 0 |
| −24829 | −24842 | −13 | 2 | 0 | 2 | 1 | 0 | 1 |
| −23228 | −23264 | −36 | 2 | 1 | 2 | 1 | 1 | 1 |
| −13440 | −13458 | −18 | 1 | 0 | 1 | 0 | 0 | 0 |
| 13083 | 13042 | −41 | 0 | 0 | 0 | 1 | 0 | 1 |
| 22933 | 22891 | −42 | 1 | 1 | 1 | 2 | 1 | 2 |
| 23877 | 23792 | −85 | 1 | 0 | 1 | 2 | 0 | 2 |
| 29164 | 29209 | 45 | 1 | 1 | 0 | 2 | 1 | 1 |
| 32991 | 33087 | 96 | 2 | 1 | 2 | 3 | 1 | 3 |
| 33277 | 33292 | 15 | 2 | 0 | 2 | 3 | 0 | 3 |
| 39134 | 39160 | 26 | 2 | 2 | 1 | 3 | 2 | 2 |
| 40975 | 40969 | − 6 | 2 | 1 | 1 | 3 | 1 | 2 |
| 42702 | 42655 | −47 | 3 | 0 | 3 | 4 | 0 | 4 |
| 42653 | 42655 | 2 | 3 | 1 | 3 | 4 | 1 | 4 |
| 44037 | 44007 | −30 | 2 | 2 | 0 | 3 | 2 | 1 |
| 49508 | 49521 | 13 | 3 | 2 | 2 | 4 | 2 | 3 |
| 50520 | 50533 | 13 | 3 | 1 | 2 | 4 | 1 | 3 |
| 52193 | 52202 | 9 | 4 | 0 | 4 | 5 | 0 | 5 |
| 52186 | 52202 | 16 | 4 | 1 | 4 | 5 | 1 | 5 |
| 61673 | 61666 | − 7 | 5 | 1 | 5 | 6 | 1 | 6 |
| 61674 | 61666 | − 8 | 5 | 0 | 5 | 6 | 0 | 6 |

sufficient to consider only the following terms of the Hamiltonian [15]:

$$H = H_R + H_{T_1} + H_{T_2} + H_{T_1T_2} + H_{RT} . \quad (3)$$

The terms $H_R$ and $H_{T_i}$ $(i=1, 2)$ stand for pure rotation and torsion vibration of top $i$, respectively; $H_{T_1T_2}$ describes the interaction between the two $CH_3$ tops and $H_{RT}$ describes the interaction between overall rotation and the torsion vibrations. In the analysis of our spectra we will ignore the $H_{RT}$ interaction term so that the rotational energy levels are merely superimposed on the energy levels of the torsion vibrations. This is permitted since in our measurements, the triplet splitting remains constant for all rotational quantum numbers. The torsional Hamiltonian consists, then, of three parts:

$$H_{T_k} = FP_{\alpha k}^2 + \tfrac{1}{2}[V_3(1-\cos 3\alpha_k) + V_6(1-\cos 6\alpha_k)] ,$$
$$k=1, 2 ,$$
$$H_{T_1T_2} = F' P_{\alpha 1} P_{\alpha 2} + \tfrac{1}{2}\{V_+[1-\cos(3\alpha_1 + 3\alpha_2)]$$
$$+ V_-[1-\cos(3\alpha_1 - 3\alpha_2)] + ...\} , \quad k=1, 2 , \quad (4)$$

where $H_{T_k}$ describes the motion of the $k$th methyl group with momentum $P_{\alpha k}$ conjugated to the torsional angle $\alpha_k$. The parameters $V_3$ and $V_6$ describe the frame–top interaction, whereas we call $V_+$ and $V_-$ the antigeared and geared top–top interactions. $F$ and $F'$ are determined by the molecular geometry

only. Note that there is a simple correspondence between our notation and that used in refs. [14,15,21]: $V_+ = \frac{1}{2}(V'_{33} - V_{33})$ and $V_- = -\frac{1}{2}(V'_{33} + V_{33})$.

Since the torsional barrier in $S_0$ is relatively low (about 250 $cm^{-1}$ [15,16], we cannot neglect the splitting caused by tunnelling. Thus, a complete analysis of the spectrum requires the use of the $G_{36}$ molecular symmetry group for the ground state, instead of $C_{2v}$. To $C_S$ symmetry of a pyramidal geometry, corresponds the symmetry group of $G_{18}$ [22]. However, the finite inversion barrier, as will be shown later, requires actually the use of $G_{36}$ also for the $S_1$ surface. The correlation between $C_{2v}$ and $G_{36}$ is reproduced in table 4, as taken from Bunker [23,24]. In the high-barrier limit, each torsional wavefunction associated with a given rotational level is ninefold degenerate. As the barrier height is lowered, this degenerate level is split into a non-degenerate $A_i$, $i \in \{1, ..., 4\}$ level, two doubly degenerate $E_i$, $i \in \{1, ..., 4\}$ levels and a fourfold degenerate G level. If the $H_{T_1T_2}$ interaction term is also neglected, the two $E_i$ states are degenerate so that torsional triplets are obtained. All low lying torsional levels actually possess this triplet structure, for reasonable assumptions concerning the torsional potential including also an $H_{T_1T_2}$ term.

Fig. 5 shows the fine structure for the (pseudo) $0_0^0$ electronic transition. The rule according to which the allowed transitions were determined is that the initial overall vibrational wavefunctions ($A_1$, $E_1$, $E_3$, G) should transform into ($A_2$, $E_1$, $E_4$, G) i.e. A↔A, E↔E, G↔G. The direct product of the irreps of the vibrational wavefunctions ($\Gamma(X_v)$) transforms as $\Gamma$(torsion)⊗$\Gamma$(wag), since all other vibrational modes are in their ground state. Therefore, it is the second inversion-tunnelling component ($\Gamma(\text{wag}) = A_2(G_{36})$) that is responsible for the observation of line 1 whereas the fine structure mainly reflects the torsion-tunnel-splitting in the ground torsional state. The

Table 4
Correlations of rotorvibrational levels of acetone. Spin statistical weights are given in parentheses

| $C_{2v}$ level | $G_{36}$ sublevels |
|---|---|
| $A_1(28)$ | $A_1(6)+E_1(4)+E_3(2)+G(16)$ |
| $A_2(28)$ | $A_3(6)+E_2(4)+E_3(2)+G(16)$ |
| $B_1(36)$ | $A_2(10)+E_1(4)+E_4(6)+G(16)$ |
| $B_2(36)$ | $A_4(10)+E_2(4)+E_4(6)+G(16)$ |

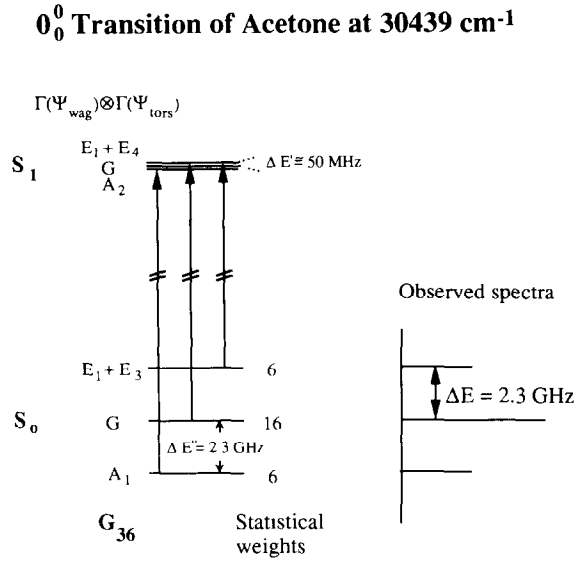


Fig. 5. Diagram showing the possible $S_1(0_1) \leftarrow S_0(0_1)$ transitions between torsional tunnel components of each rotational level for the case where the splitting in the excited state is small. Only three lines can be experimentally observed in this case. The structure of each triplet is shown on the right side

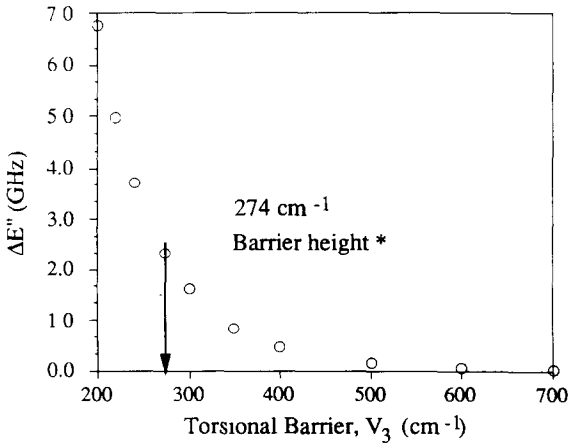


Fig. 6. Tunnel splitting as a function of torsional barrier height in the ground state.

triplet splitting of the lines in the observed spectrum, $\Delta E = |\Delta E' - \Delta E''|$, is determined by the difference in torsional energy splittings in the upper and lower electronic states. Fig. 6 shows our calculation of the

expected energy splitting, $\Delta E''$, as a function of the barrier height. It is found that 2.3 GHz is compatible with a barrier of about 250 $cm^{-1}$, as observed by microwave spectroscopy. Assuming that the splitting in the excited state is smaller than our accuracy ($\approx 50$ MHz) we estimate a lower limit for the barrier height ($V_3$) to internal rotation in the $S_1$ state to be around 600 $cm^{-1}$. A more precise estimate is deferred to the analysis of the torsional energy levels.

The observed triplet intensities obey the ratio 1:2:1, within the experimental uncertainty, which is in agreement with predictions based upon spin statistics, see fig. 5.

### 3.2. Refined analysis of the $0_0^0$ band

The torsional energy levels and wavefunctions are well known for the case of two-top molecules [25,21]. The product of single-top wavefunctions serves as the basis for the total two-top Hamiltonian (using the principal axis method (PAM)):

$$U^{v_1 v_2}_{\sigma_1 \sigma_2}(\alpha_1, \alpha_2) = U^{v_1}_{\sigma_1}(\alpha_1) U^{v_2}_{\sigma_2}(\alpha_2) , \qquad (5)$$

where

$$U^{v}_{\sigma}(\alpha) = \sum_{k=-\infty}^{\infty} A_k^{\{v\}} \exp[i(3k+\sigma)\alpha] . \qquad (6)$$

The label $v$ is called the principal torsional quantum number since it becomes the quantum number for the limiting harmonic oscillator ($V_3 \to \infty$). The index $\sigma = 0, \pm 1$ gives the symmetries of the wavefunctions and thus distinguishes between the tunnelling sublevels. Each eigenstate of the two-top torsional Hamiltonian is characterized by the four quantum numbers $v_1, \sigma_1, v_2, \sigma_2$. In a somewhat simplified picture, $v_1$ and $v_2$ denote the number of torsional quanta present in each top while the various combinations of $\sigma_1$, $\sigma_2$ provide the overall nine-fold degeneracy of the torsional level.

The out-of-plane wagging mode ($\nu_{23}$, $b_1$) can be viewed as the motion of the central C atom with respect to the plane spanned by the two methyl groups and the O atom. Considering first the C=O out-of-plane wagging we have calculated the double well potential fitting our observed spectra using the tables of Coon et al. [26]. The results are shown in fig. 7. In $C_{2v}$, the symmetry of the vibrational levels alternates between $A_1$ and $B_1$, and thus only half of the levels

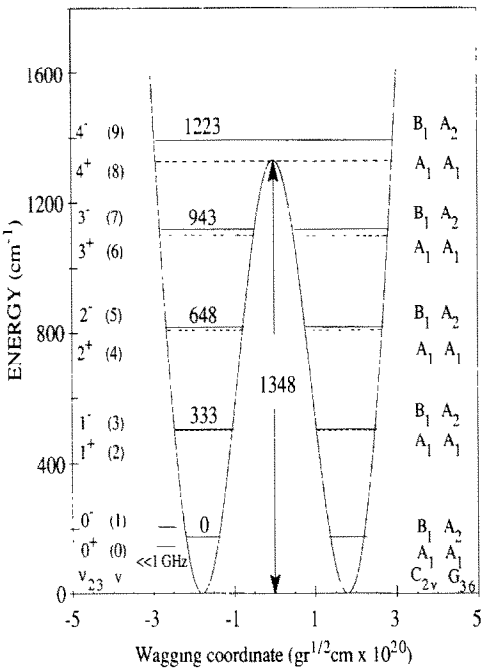


Fig. 7. The calculated out-of-plane wagging potential of $S_1$. The parameters used in the calculation are $\rho = 1.20$, $B = 6.0$, $v_0 = 224.6$ $cm^{-1}$ (see ref. [26]). Only odd levels ($A_2$ in $G_{36}$) can be accessed for zero-torsion, the forbidden ones are shown by dashed lines. The splitting of the lowest level is much smaller than 1 GHz and amounts to 1, 17 and 270 GHz, respectively, for the next higher ones. The position of levels is given in wavenumbers.

will be observed in the excitation spectrum. For a reasonable potential model the barrier height obtained – 1348 $cm^{-1}$ – was made to fit the transition at 333 $cm^{-1}$ (line 5, see table 2). It leads to a splitting of about 1 GHz, due to tunnelling, between the two levels $v=2$ and $v=3$ ($1^+$ and $1^-$). The lowest doublet splits $\ll 1$ GHz.

Since the energy, $E(23^1)$, of the C=O out-of-plane wagging is only some GHz above the value of $E(23^0)$, we propose to consider its coupling with the torsional motion. In turn, this coupling will allow transitions to some of the forbidden levels, as required by the appearance of quintets in higher members of the torsional progression. The wagging motion will be described by the distance coordinate, $q_w$. As follows from the character table of $G_{36}$, a translation along this direction belongs to the $A_2$ irreducible representation, as does the gearing motion of the two $CH_3$ groups. In order to couple the two kinds of motion we look for

a potential term – of $A_1$ symmetry – that contains naturally the coordinates of both. The operator, to be added to our Hamiltonian (4),

$$V_{\text{coupl}} = C_{\text{coupl}} q_w \sin(3\alpha_1 - 3\alpha_2) , \quad (7)$$

offers itself since both factors are of $A_2$ symmetry with $A_2 \otimes A_2 = A_1$. Note that positive torsional angles $\alpha_1$ and $\alpha_2$ are defined as clockwise rotation looked from the central C atom; i.e. the minus sign in the argument of the sine factor corresponds to the gearing operation of $A_2$ symmetry. Having thus established the simplest potential coupling term between wagging and torsion, we next consider qualitatively its influence on the possible transitions between energy levels. Without this coupling the excitation leads – for the $0_0^0$ band – from the $S_0$ ground state to the electronically excited state with one vibrational quantum in the wagging mode, $23^1$. For instance, the initial quadruplet of states ($A_1$, $E_1$, $E_3$, G) is excited to the quadruplet ($A_2$, $E_1$, $E_4$, G) = $A_2 \otimes (A_1, E_1, E_3, G)$. (Note that the transition dipole operator is of $A_2$ symmetry.) This would apply to the $0_1$ as well as to the allowed excitations of $2_1$ and $2_3$ levels.

With the coupling term (7), two members of the quadruplet of excited states just discussed, ($A_2$, $E_1$, $E_4$, G), appear to be coupled to two members of the slightly lower quadruplet of states, ($A_1$, $E_1$, $E_3$, G) of $23^0$, i.e. $E_1$ with $E_1$ and G with G. Note that this coupling leads to five energetically distinct transitions, $A_1 \rightarrow A_2(23^1)$, $E_1 \rightarrow E_1(23^1)$ and $E_3 \rightarrow E_4(23^1)$, $E_1 \rightarrow E_1(23^0)$, $G \rightarrow G(23^1)$ and $G \rightarrow G(23^0)$. The resulting pattern is thus a quintet, as it is observed for most bands but *not* for the $0_0^0$ band.

In the following we will show why the proposed coupling vanishes for the $0_0^0$ transition so that the spectrum possesses a triplet structure while the "direct" and "coupled" transition strength in the spectra of bands 2, 4 and 6 display quintet structure, whose components are of similar intensity. A transition is called "direct", if the final level (with torsional splitting being neglected) has $B_1$ symmetry, in $C_{2v}$, and can thus be reached through a $B_2$ transition dipole moment, see eq. (2). "Coupled" transition needs eq. (7) to become allowed. The matrix element of the coupling may be expressed as

$$\langle \Psi_{v=0}(q_w) U^{00}_{\sigma_1\sigma_2}(\alpha_1, \alpha_2) | q_w \sin(3\alpha_1 - 3\alpha_2) | \Psi_{v=1}(q_w) U^{00}_{\sigma_1\sigma_2}(\alpha_1, \alpha_2) \rangle , \quad (8)$$

where $\Psi_{v=0}(q_w)$ and $\Psi_{v=1}(q_w)$ are the part of the bra and ket describing the lowest and first excited wagging states split by the tunneling motion and $U(\alpha_1, \alpha_2)$ – the torsional part (see eq. (5)). The coupling between $v=0$ and $v=1$ wagging levels is realized by the factor $q_w$ in $V_{\text{coupl}}$. The torsional coupling takes place through the sine term of $A_2$ symmetry. If the sine term is written as a difference of two exponentials, it becomes evident that raising the degree of torsional excitation of one internal top is accompanied by lowering the torsional excitation of the other one. For the torsional ground state, this operation necessarily yields zero, i.e. the observed triplet structure of the $0_0^0$ band agrees with our analysis even after introduction of $V_{\text{coupl}}$, eq. (7).

### 3.3. Analysis of the torsional progression

Table 5 lists the lowest torsional states with their tunneling symmetries in $G_{36}$. In the middle column, those states are indicated which cannot be excited from the ground state of acetone ($A_1$ vibronic symmetry, $A_1$, $E_1$, $E_3$, G torsional symmetries).

The progression bands at 0, 172.5, 314.5, 346.3, 474.3, 510 and 640.8 $cm^{-1}$ are assigned to the antigearing and gearing torsional modes $\nu_{12}$ and $\nu_{24}$ (see table 6). The torsional energy levels calculated by diagonalizing the Hamiltonian (eq. (4)) are depicted in fig. 8 together with the experimental energies. The kinetic energy coefficient $F^v$ was taken as a parameter along with the potential parameters $V_3$, $V_6$, $V_+$ and $V_-$, since only qualitative information is available on the excited state geometry. The best calculation resulted in an agreement within 2 $cm^{-1}$ between the experimental and calculated frequencies of the lines 2, 4, 6. Each of the lines 2, 4, 6 has a quintet fine structure which is constant for all the rotational lines within a given band. The remaining discrepancy, and the fact that the bands display quintet fine structure (rather than triplet, like in the $0_0^0$ band) may be accounted for by introducing a coupling between the torsional motion and other vibrational modes. Thus, to the torsional Hamiltonian (eq. (4)) the coupling term, $V_{\text{coupl}}$, eq. (7), will be added.

For instance, we have ($A_1$, $E_1$, $E_3$, G) = $A_2 \otimes (A_2$, $E_1$, $E_4$, G) yielding an additional doublet of $E_1$ and G symmetry as final levels if the excitation of the $1_2$ torsional level is accompanied by excitation of the wag-

Table 5
Symmetries of lower torsional vibrational states of acetone in the $S_1$ excited state with their tunneling sublevels

| $N_k$ [a] | $v^+$ | $v^-$ | $G(C_{2v})$ | Selection rules based on $C_{2v}$ | $G(G_{36})$ [b] | |
|---|---|---|---|---|---|---|
| | | | | | $\Gamma_{tors}\otimes A_1$(wag) | $\Gamma_{tors}\otimes A_2$(wag) |
| $0_1$ | 0 | 0 | $A_1$ | | $A_1+E_1+E_3+G$ | $(A_2+E_1+E_4+G)$ |
| $1_1$ | 1 | 0 | $A_2$ | forbidden | $A_3+E_2+E_3+G$ | $(A_4+E_2+E_4+G)$ |
| $1_2$ | 0 | 1 | $B_1$ | | $A_2+E_1+E_4+G$ | $(A_1+E_1+E_3+G)$ |
| $2_1$ | (2 | 0) | $A_1$ | | $A_1+E+E_3+G$ | $(A_2+E_1+E_4+G)$ |
| $2_2$ | (1 | 1) | $B_2$ | forbidden | $A_4+E_2+E_4+G$ | $(A_3+E_2+E_3+G)$ |
| $2_3$ | (0 | 2) | $A_1$ | | $A_1+E_1+E_3+G$ | $(A_2+E_1+E_4+G)$ |
| $3_1$ | (3 | 0) | $A_2$ | forbidden | $A_3+E_2+E_3+G$ | $(A_4+E_2+E_4+G)$ |
| $3_2$ | (2 | 1) | $B_1$ | | $A_2+E_1+E_4+G$ | $(A_1+E_1+E_3+G)$ |
| $3_3$ | (1 | 2) | $A_2$ | forbidden | $A_3+E_2+E_3+G$ | $(A_4+E_2+E_4+G)$ |
| $3_4$ | (0 | 3) | $B_1$ | | $A_2+E_1+E_4+G$ | $(A_1+E_1+E_3+G)$ |
| $4_1$ | (4 | 0) | $A_1$ | | $A_1+E_1+E_3+G$ | $(A_2+E_1+E_4+G)$ |
| $4_2$ | (3 | 1) | $B_2$ | forbidden | $A_4+E_2+E_4+G$ | $(A_3+E_2+E_3+G)$ |
| $4_3$ | (2 | 2) | $A_1$ | | $A_1+E_1+E_3+G$ | $(A_2+E_1+E_4+G)$ |
| $4_4$ | (1 | 3) | $B_2$ | forbidden | $A_4+E_2+E_4+G$ | $(A_3+E_2+E_3+G)$ |
| $4_5$ | (0 | 4) | $A_1$ | | $A_1+E_1+E_3+G$ | $(A_2+E_1+E_4+G)$ |

[a] $N=v^++v^-$ (number of torsional quanta). The group of levels having the same $N$ is defined as a torsional polyad. Polyad $N$ consists of $N+1$ levels labeled by $k$. The $v^+$, $v^-$ designation here refers to the gearing and antigearing torsional fundamentals but not to the actual distribution of energy between the two tops. Starting from the second polyad onwards the $v^+$, $v^-$ designation is put into parenthesis since the actual motion described by the eigenfunctions has a more complicated character.

[b] The left term is the representation of the torsional states coupled to the $A_1$ component of the out-of-plane wagging tunnel-split component, the right hand term (in parentheses) is the representation of the same torsional state coupled to the $A_2$ component.

Table 6
Comparison of experimental and calculated torsional frequencies [a]

| $N_k$ | Calculated [b] | Experimental [c] (line #) | $\Delta$ [d] | |
|---|---|---|---|---|
| | | | A–G | E–G |
| $1_1$ | 155.5 | not observed | 0.255 | 0.255 |
| $1_2$ | 173.9 | 172.5 (2) | 0.328 | 0.328 |
| $2_1$ | 314.7 | 314.5 (4) | 2.3 | 2.3 |
| $2_2$ | 324.0 | not observed | 5.0 | 5.0 |
| $2_3$ | 344.7 | 346.3 (6) | 2.417 | 2.390 |
| $3_1$ | 471.2 | not observed | 54.1 | 10.4 |
| $3_2$ | 474.0 | 474.3 (8) | 21.7 | 64.5 |
| $3_3$ | 489.0 | not observed | 16.9 | 17.7 |
| $3_4$ | 511.9 | 510 (10) | 5.28 | 5.44 |
| $4_1$ | 597.0 | 598 (12,12a) | 0.796 | 510 |
| $4_2$ | 614.0 | not observed | 509 | 0.07 |
| $4_3$ | 641 | 640.8 (14a) | 13 | 9.9 |
| $4_4$ | 646 | not observed | 26.3 | 28.8 |
| $4_5$ | 673 | | | |

[a] Frequencies are in $cm^{-1}$; measured above the $0_0^0$ band ($\nu_0=30439.9145\ cm^{-1}$); the $0_1$ is calculated to be at $164.4\ cm^{-1}$.

[b] Parameters used in calculation: $F=5.7255\ cm^{-1}$, $F'=-0.28128\ cm^{-1}$, $V_3=832.03\ cm^{-1}$, $V_6=-60.3\ cm^{-1}$, $V_+=13.46\ cm^{-1}$, $V_-=-86.63\ cm^{-1}$.

[c] The band origin is given where a fit was possible; otherwise, the estimated center of the band is given.

[d] Calculated maximum splitting between the A, E and G sublevels in GHz. It is noted that the degeneracy between the pairs of E levels for a given $N_k$ level prevails and is lifted to 15 MHz only in $4_5$. For $N_k=1_2$, an experimental splitting $\Delta_{EG}=0.3$ GHz has been assigned.

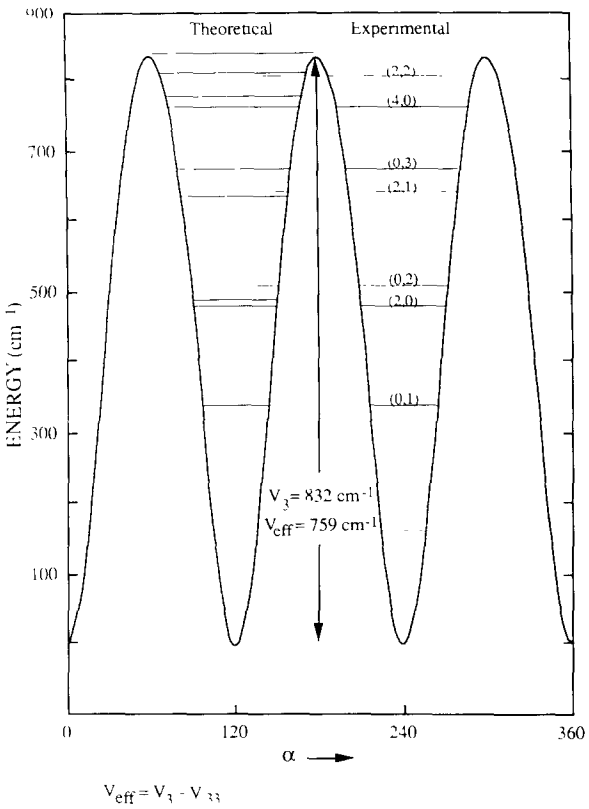


Fig. 8. The calculated torsional potential for the excited state and the associated energy levels. Unobserved levels are not shown on the right side.

ging mode (see fig. 9 and table 5). The effect of the very small splitting ($\ll$1 GHz) between the two lowest wagging levels is that torsional sublevels of the same symmetry, i.e. G with G and E with E are coupled by the $V_{coupl}$ term. The resulting pattern is a quintet, instead of a doublet. In our assignments we were guided by the nearly constant ($\approx$3.2 GHz) distance between the two strongest lines within the quintets. Our analysis implies then that the strength of the interaction caused by the $V_{coupl}$ term is of the order of 2 GHz.

Linear combinations of eq. (5) form the eigenfunctions of our torsional Hamiltonian. The same basis functions have been used and are discussed in ref. [27]. As an example of an excited state, the $1_2$ torsional level may be described with a high accuracy by the eigenfunction $(1/\sqrt{2})$ $(|1,0\rangle - |0,1\rangle)$ where $|v_1, v_2\rangle$ indicates $v_1$ and $v_2$ torsional quanta in top1 and top2, respectively. Substitution of this expression into the matrix element of eq. (8) results in a nonvanishing torsional coupling: the $\sin(3\alpha_1 - 3\alpha_2)$ operator working upon $(|1,0\rangle - |0,1\rangle)$ yields e.g. $(|0,1\rangle - |1,0\rangle)$ and thus a nonvanishing coupling matrix element is obtained. Within the torsional multiplet we find a wagging mixture ($23^0$ and $23^1$) through $V_{coupl}$, eq. (7), yielding transitions which were forbidden before. In an analogous way the "coupled" transitions in the bands at 314.5 and 346.3 cm$^{-1}$ become allowed. The intensities of the "direct" and "coupled" transitions are nearly equal. This fact implies that the unperturbed eigenfunctions mix with nearly equal weights. It is the near degeneracy of the $23^0$ and $23^1$ levels that makes such a mixing possible. We can easily show (see ref. [28]) that if the unperturbed wagging levels are tunnel-split by 1 GHz, a coupling strength on the order of 2 GHz would be enough to bring the intensity of a "coupled" transition to about 40% of the "direct" one. A full treatment must be based on a Hamiltonian including the $V_{coupl}$ term.

For the third and fourth polyads only a preliminary analysis can be presented. The band around 474 cm$^{-1}$ (line 8) spreads over $\approx$12 cm$^{-1}$, compared to $\approx$8 cm$^{-1}$ for the nearby lying lines 7 and 9. The prediction of an exceptionally large ($\approx$2 cm$^{-1}$) torsional splitting within the $3_2$ level (table 6) agrees with the large shifts ($\approx$4 cm$^{-1}$) between various components found in a preliminary analysis of line 8. The band at 510 cm$^{-1}$ (line 10) is assigned to the $3_4$ level. Both $3_2$ and $3_4$ bands are expected to have a quintet fine structure. Line 10 exhibits higher than a triplet fine structure, whereas line 8 is much more complicated. The rotational analysis of line 8 and all other higher energy lines is complicated by the fact that different components within the same band have, at times, different rotational constants. We assign lines 12 and 12a to the $4_1$ level. Line 12a was measured with 0.2 cm$^{-1}$ resolution only [6]. It is a relatively broad band, similar to line 8 and can, therefore, accommodate the needed calculated $\approx$17 cm$^{-1}$ split, $\Delta_{EG}$ (see table 6). Line 14a, at 641 cm$^{-1}$, fits well to the assignment $23^1+4_3$; in table 7 it is remarked that the nature of the eigenfunctions has the symmetry of (2*antigearing+2*gearing). Note that the eigenfunction may differ from the mixture be-

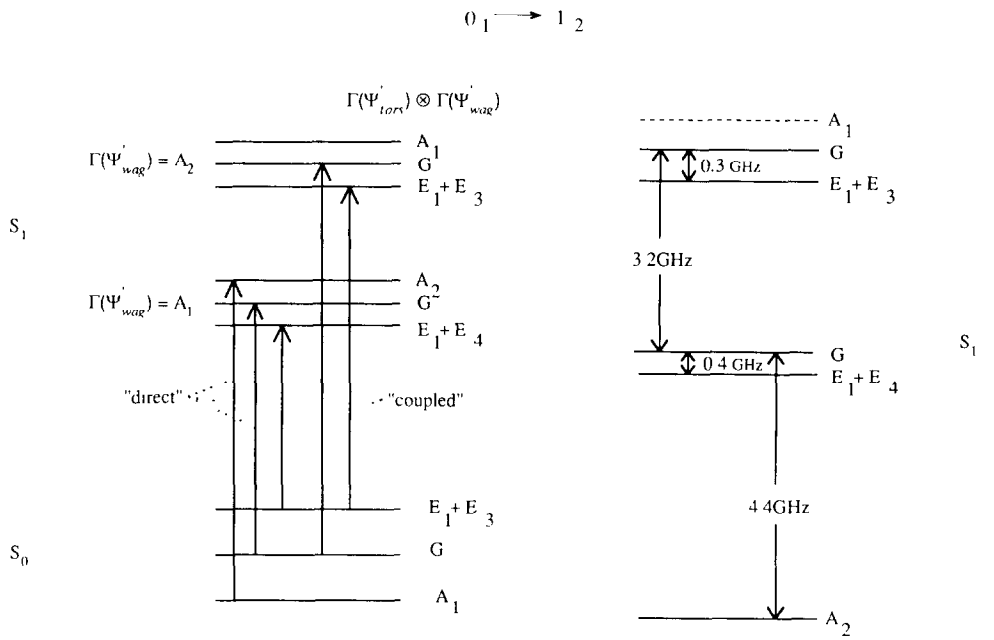


Fig. 9. Level scheme for the $S_1$ $(1_2)$←$S_0$ $(0_1)$ transition in acetone. Indicated are the "direct" transitions to the lowest wagging component and the "coupled" transitions to the higher wagging component. Also indicated are the energy splittings on the $S_1$ $(1_2)$ level as deduced from the observed spectrum.

longing to $n*$antigearing$+n*$gearing in case that a parenthesis occurs in the last column of table 7. Up to the second polyad, however, such a characterization is rather accurate. It is evident that the analysis of these and higher levels may require introduction of more coupling terms.

### 3.4. Other low lying modes

In the ground state, three other low frequency modes are known (table 1): $\nu''_8$, the C–C–C bend at 385 $cm^{-1}$, $\nu''_{23}$, the C=O out-of-plane wagging at 484 $cm^{-1}$ and $\nu''_{19}$, the C=O in-plane-wagging at 530 $cm^{-1}$. For the $S_1$ state we offer two possible assignments below, to explain our spectra, see table 8. In both cases $\nu'_8 = 373$ $cm^{-1}$. Further, $\nu'_{23} = 333$ $cm^{-1}$ and $\nu'_{19} = 621$ $cm^{-1}$, for the second possibility and $\nu'_{19} = 177$ $cm^{-1}$ and $\nu'_{23}$ undetermined, for the first and by us preferred possibility, as will discussed next in connection with the $*$, $**$ and $***$ progressions of table 7.

#### 3.4.1. Single star progression

*First possibility.* The bands at 333.5, 487, 624, 624 and 645 $cm^{-1}$ (lines 5, 9, 13a, 13b and 14b, respectively) are assigned to the $\nu'_{19}$+torsion progression. The C=O in-plane-wagging, $\nu'_{19}(A_4)$, can have an a-type spectrum only if coupled with the antigearing $\nu_{12}(A_3)$ and is expected to have a quintet fine structure. Line 5 at 333 $cm^{-1}$ is assigned to $19^1+1_1$ and displays a quintet (see fig. 4b). This assignment suggests a very big change in the frequency of the C=O in-plane wagging, i.e. 177 $cm^{-1}$ in $S_1$, compared to 530 $cm^{-1}$ in $S_0$ (table 1). Lines 9, 13b, and 14b are assigned to $19^1+2_2$, $19^1+3_1$, and $19^1+3_3$, respectively. It follows from this assignment that the torsional antigearing motion possesses an intermode anharmonicity of about 20 $cm^{-1}$ between $\nu_{19}$ and $\nu_{12}$.

*Second possibility.* The single starred progression is assigned to the C=O out-of-plane motion. Line 5 (333 $cm^{-1}$) is assigned to $23^3$, the upper tunnel-split level of the second dyade of the wagging mode. The quintet fine structure of the band with 3.2 GHz distance between the two strongest components implies that the two levels ($23^3$ and $23^2$) are almost degenerate (split by less than 1 GHz). The "coupled" transition to the $23^2$ level, however, actually is not coupled by eq. (7), because we deal here with the torsional

Table 7
Assignment of the long-wavelength bands observed in the fluorescence excitation spectrum of acetone. For line 8 onwards, assignments and analysis are less certain

| Line # | Energy [a] ($cm^{-1}$) | Assignment [b] | | Remarks [c] |
|---|---|---|---|---|
| | | ref. [1] | this work [d] | |
| 1 | 0[e] | $\nu_{23}^{0+}$ | $23^1$ | |
| 2 | 172.5 | (1,0) | (0,1) | gearing ($A_2$) |
| 3 | hot band | | not observed | |
| 4 | 314.5 | (2,0) | $23^1+(2,0)$ | 2*antigearing ($A_2$) |
| 5 | 333.6 | (2,0) | * | two possible assignments, see text |
| 6 | 346.3 | (1,1) | $23^1+(0,2)$ | 2*gearing ($A_2$) |
| 7 | 373 | $\nu_{23}^{1+}$ | ** | |
| 8 | 474 | (3,0) | (2,1) | (gearing+2*antigearing ($A_2$)) |
| 9 | 487 | (2,1) | * | |
| 10 | 510 | (2,1) | (0,3) | (3*gearing ($A_2$)) |
| 11 | 544 | $\nu_{23}^{1+}+(1,0)$ | ** | |
| 12 | 578 | $\nu_{23}^{1-}$ | $23^1+(4,0)$ | (4*antigearing ($A_2$)) |
| 12a | 598 | [f] | $23^1+(4,0)$ | [g] |
| 13a | 621 | | * or *** | |
| 13b | 624 | (4,0) [h] | * | |
| 14a | 641 | | (2,2) | (2*gearing+2*antigearing ($A_2$)) |
| 14b | 645 | (3,1) [h] | * | |

[a] Energy above the origin of $S_1$.
[b] Torsional quanta are listed as $(t,j)$ where $t$ and $j$ are the number of quanta excited in the antigearing and gearing motions respectively.
[c] Symmetry species are in $G_{36}$.
[d] *, **, *** are (starting levels of) new torsional series; for their assignment see text.
[e] The zero-point energy level of the CO out-of-plane wagging ($23^0$) is forbidden for a dipole transition from the $S_0$ vibrationless level. The first overtone ($23^1$) is calculated to be 1.1 GHz above $23^0$ and is the pseudo-origin of the observed spectrum.
[f] Not mentioned in ref. [1], was measured with 0.2 $cm^{-1}$ resolution in ref. [2] (see fig. 1).
[g] Belongs, too, to $N=4$ and $k=1$; for its large splitting, see table 6. $\Delta_{EG}=17$ $cm^{-1}$.
[h] Lines 13 and 14 consist of two nearly overlapping lines and were given one assignment in ref. [1].

Table 8
Low energy modes of acetone ($cm^{-1}$)

| | $S_0$ | $S_1$ | |
|---|---|---|---|
| | | first possibility | second possibility |
| $\nu_{12}$ torsion (antigearing) | 77 | 155.5 | 155.5 |
| $\nu_{24}$ torsion (gearing) | 124 | 172.5 | 172.5 |
| $\nu_8$ C–C–C bend | 385 | 373 | 373 |
| $\nu_{23}$ C=O out-of-plane wagging | 484 | – | 333 |
| $\nu_{19}$ C=O in-plane-wagging | 530 | 177.5 | 465.4 |
| wagging barrier height | – | 927 | 1350 |
| effective torsional barrier | 270 | 759 | 759 |

ground state. We were not able to individuate an alternative coupling mechanism so far to explain the observed quintet (and therefore prefer the first possibility). For line 9, 13b and 14b the assignment becomes $23^2+1_2$ at 484 $cm^{-1}$, $23^3+2_1$ at 624 $cm^{-1}$ and $23^3+2_3$ at 645 $cm^{-1}$. In all cases, quintets are expected and found for the first two, in our preliminary analysis. These assignments (especially of lines 9 and 13b) necessitate a wagging barrier of about 1350 $cm^{-1}$.

*3.4.2. Two stars progression*

The band at 373 $cm^{-1}$ (line 7) is assigned to the C–C–C bending, $\nu_8$ for both possibilities. The $A_1$ symmetry $\nu_8$ is expected to have a triplet fine structure, just as the $0_0^0$ band. The observed spectrum of line 7 has a triplet fine structure as shown in fig. 4d with a consistent 2.1 GHz splitting of each rotational line and approximately 1:2:1 relative intensities. The 200 MHz decrease from the 2.3 GHz triplet splitting in the $0_0^0$ band is four times our experimental accuracy. We argue that since the 373 $cm^{-1}$ band serves as a pseudo-origin for the progression of $8^1$+torsion combination bands, the torsional barrier used in the torsional energy-level calculations for the excited state must be lowered. Fig. 6 shows that a 200 MHz zero-tunnel-splitting is obtained for $V_3 = 450$ $cm^{-1}$, i.e. the torsional barrier is effectively lowered by nearly the amount of vibrational excitation. The physical reason for such an effect might be that a somewhat different equilibrium geometry of acetone in the $8^1$ vibrationally excited state lowers the hindrance of the two $CH_3$ groups.

*3.4.3. Three stars progression*

*Second possibility.* The band at 621 $cm^{-1}$ (line 13a) is assigned to $\nu'_{19} + 1_1$. We were able to fit line 13a to an a-type rotational transition with $\nu_0 = 31061.6781$ $cm^{-1}$ ($\Delta E = 621.7636$ $cm^{-1}$) (see table 2). It is one of the strongest lines measured in this work and our preliminary analysis shows that establishment of the fine structure, even at this high vibrational excitation, is possible. In the first possible assignment, this *** line 13a belongs to the * series, assigned as $19^1 + 3_1$. It belongs to the same component of a polyad, $3_1$, as line 13b, with a calculated splitting of about 1 $cm^{-1}$.

## 4. Discussion

The high resolution spectra reported in this work led to the proposal of an effective barrier height for torsion – 759 $cm^{-1}$ in the $S_1$ state. The torsional barrier is much larger than that in the ground state, and leads to a much smaller frequency difference between the torsional fundamentals – the calculated separation between the (0, 1) and (1, 0) levels is 18.4 $cm^{-1}$, compared to 63 $cm^{-1}$ in the ground state. The high barrier may be related to the fact that the two rotors are somewhat closer to each other due to the bent configuration of the excited state. Internal rotational barriers are believed to reflect electronic densities in the bands adjacent to the rotor [29,30]. The n,$\pi^*$ transition involves an increase in the electronic density of the C=O bond which could increase also the density in the C–C bond (by hyperconjugation), making the bond stiffer and rising the barrier. These speculations should be checked by electronic density calculations.

The inversion barrier of the $S_1$ state – 1348 $cm^{-1}$ – is much larger than that of formaldehyde (350 $cm^{-1}$) and acetaldehyde (541 $cm^{-1}$), probably reflecting the increased stabilization of the pyramidal form upon exchange of a hydrogen atom by a methyl group.

Our analysis of the low energy torsional bands makes it compulsory to include an additional potential coupling term, $V_{coupl}$, into the Hamiltonian. Doing that, we, nevertheless, interpret the spectra using the $G_{36}$ molecular symmetry group for acetone in the $S_1$ electronic state.

Durig and co-workers developed a general theory for molecules with two internal rotors of $C_{3v}$ symmetry and showed how it may be utilized for several different models [31,32]. They recognized the difference of the torsional Hamiltonians between the models of $C_{2v}$ and $C_S$ molecules with two equivalent tops ($C_{2v}(e)$ and $C_S(e)$ in their notation) but also pointed out their formal identity. In particular, this difference manifested itself by inclusion of more potential terms into the Hamiltonian describing the torsional motion of a molecule having $C_S(G_{18})$ symmetry. One of them, of $A_1$ symmetry in $G_{18}$, is

$$V''_{33} \sin(3\alpha_1 - 3\alpha_2) \qquad (11)$$

(compare to eq. (7)). Acetone in the ground $S_0$ state corresponds to the $C_{2v}(e)$ model. According to the classification of Durig et al., in case the wagging tunnelling is frozen acetone in the excited $S_1$ state should be treated within the $C_S(e)$ model since it attains a pyramidal equilibrium geometry. That is, if we assume for a moment an infinite inversion barrier, there are two equivalent potential minima corresponding to two bent (rigid) conformations of $C_S(G_{18})$ symmetry. These minima are distinguished by a simul-

taneous change of the signs of the two coordinates: $q_w$ for the wagging and $3\alpha_1 - 3\alpha_2$ for the gearing torsion. The term, eq. (11), must be included in the torsional Hamiltonian. The $C_S(e)$ model was applied to the analysis of the Raman spectra of dimethylamine where the tunnelling of the H atom through the CNC plane was thought to be frozen [21]. If we lower now the inversion barrier the tunneling motion becomes feasible and the levels split, for the two cases. Performing a tunnelling through the barrier is equivalent to adding a new symmetry operation–reflection through the CCC plane – which is absent in the $G_{18}$ symmetry group and belongs to the $A_2$ irrep in $G_{36}$. The wavefunctions describing the wagging motion are written as symmetric and antisymmetric linear combinations of $\Psi(+q_w)$ and $\Psi(-q_w)$. A feasible tunnelling through the inversion barrier rises the symmetry of the molecule and, in our case, allows to treat the internal rotation of acetone($S_1$) within $G_{36}$.

Thus, in our analysis we introduce a coupling between the CO out-of-plane wagging ($\nu_{23}$) and torsional modes. The physical origin lies in the fact that for certain ($\alpha_1$, $\alpha_2$) configurations the inversion motion brings the molecule to a nonequivalent configuration if a simultaneous adjustment of ($\alpha_1$, $\alpha_2$) is not allowed. The proposed coupling term of eq. (7) leaves the Hamiltonian invariant under the operations of the $G_{36}$ symmetry group, being a product of two terms, both antisymmetric with respect to inversion through the CCC plane.

The fact that the transitions observed are a-type, as well as the observed splitting patterns led to some reassignment of the vibrational bands observed in the excitation spectrum. Table 7 summarizes the situation. In contrast to ref. [1], we assign the first band to the upper fine structure component of the tunnel split wagging motion. Thus, it is not necessary to invoke second order perturbation theory in order to account for intensity borrowing that makes the transition allowed. As in formaldehyde, this $B_1$ type vibration mixes the $n\pi^*(A_2)$ state with the $n\sigma^*(B_2)$ state.

The occurrence of b-type transitions in the spectra cannot be entirely ruled out, since a full analysis is yet to be completed. B-type transitions are expected for vibrations having $A_2(C_{2v})$ symmetry. However, up to line 7, at 373 $cm^{-1}$, all lines exhibit pure a-type rotational transitions.

It is clear from our calculations that many torsional bands are forbidden. Our successful assignment is an a posteriori support for the use of the $C_{2v}$ molecular point group rather than $C_S$.

The n,$\pi^*$ excitation leads to considerable changes in the frequencies of some low energy mode frequencies of acetone (table 8). Though, for the torsion–vibrational combination bands we prefer the "first possibility" of table 8, the change $\nu''_{19} = 530$ $cm^{-1} \rightarrow \nu'_{19} = 177$ $cm^{-1}$ is discomfortingly large and should fill us with caution. Remember, however, that acetone changes its geometry for the transition $S_1 \leftarrow S_0$ which permits relatively big changes of mode frequencies. In addition, for the related acetaldehyde molecule the corresponding shift is also very large, $\nu''_{10} = 509$ $cm^{-1} \rightarrow \nu'_{10} = 370$ $cm^{-1}$ [33]. In conclusion, the first possible assignment is the favoured but still tentative one.

## References


[1] J.A. Pople and J.W. Sidman, J. Chem. Phys. 27 (1957) 1270.
[2] V.A. Job, V. Sethuraman and K.K. Innes, J. Mol. Spectry. 30 (1969) 365.
[3] E.F. Worden Jr., Spectrochim. Acta 22 (1966) 21.
[4] D.J. Clouthier and D.A. Ramsey, Ann. Rev. Phys. Chem. 34 (1983) 31.
[5] M. Baba, I. Hanazaki and U. Nagashima, J. Chem. Phys. 82 (1985) 3938.
[6] H. Zuckermann, B Schmitz and Y. Haas, J Chem. Phys. 93 (1989) 4083.
[7] H. Zuckermann and Y. Haas, unpublished.
[8] J.G. Philis, J.M. Berman and L. Goodman, Chem. Phys. Letters 167 (1990) 16.
[9] P. Groner, G.A. Guirgis and J.R. Durig, J. Chem. Phys. 86 (1987) 565.
[10] T. Shimanouchi, Tables of molecular vibrational frequencies, NSRDS-NBS 39 (1987).
[11] P. Cossee and J.H. Schachtschneider, J. Chem. Phys. 44 (1966) 97.
[12] W.C. Harris and I.W. Levin, J. Mol. Spectry. 43 (1972) 117.
[13] R. McDiarmid and A. Sabljic, J. Chem. Phys. 89 (1988) 6086.
[14] A.G. Ozkabak, J.G. Philis and L. Goodman, J. Am. Chem. Soc. 112 (1990) 7854. [Note that these authors use a different coordinate system than the one used in this paper. Their $\nu_{17}(b_2)$ corresponds to our $\nu_{24}(b_1)$.]
[15] J.D Swalen and C.C. Costain, J. Chem. Phys. 31 (1959) 1562.
[16] R. Nelson and L. Pierce, J. Mol Spectry. 18 (1965) 344.
[17] R. Peter and H. Dreizler, Z. Naturforsch. A 20a (1965) 301.
[18] J.M. Vacherand, B.P. van Eijck, J Burie and J Demaison, J. Mol. Spectry. 118 (1986) 355.

[19] E. Cromwell, T. Trickl, Y.T. Lee and A.H. Kung, Rev. Sci. Instr. 60 (1989) 2888.
[20] S. Gerstenkorn and P. Luc, Atlas du spectroscopie d'absorption de la molecule d'iode (CNRS, 1978).
[21] C.C. Lin and J.D. Swalen, Rev. Mod. Phys. 31 (1959) 841.
[22] R. Engeln, J. Reuss, D. Consalvo, J.W.I. van Bladel and A. van der Avoird, Chem. Phys. Letters 170 (1990) 206.
[23] P.R Bunker, Molecular symmetry and spectroscopy (Academic Press, New York, 1979)
[24] P.R. Bunker, in: Vibrational spectra and structure, Vol. 3, ed. J.R. Durig (Dekker, New York, 1975).
[25] R.J. Myers and E.B. Wilson Jr., J. Chem. Phys. 33 (1960) 186.
[26] J.B. Coon, N.W. Naugle and R.D. McKenzie, J. Mol. Spectry. 20 (1966) 107.
[27] R. Engeln, J. Reuss, D. Consalvo, J.W.I. van Bladel, A. van der Avoird and V. Pavlov-Verevkin, Chem. Phys. 144 (1990) 81.
[28] C.H. Townes and A.L. Shawlow, Microwave spectroscopy (McGraw-Hill, New York, 1955) ch. 2, p. 38.
[29] X.Q. Tan, W.A. Majewski, D.F. Plusquellic and D.W. Pratt, J. Chem. Phys. 94 (1991) 7721.
[30] X.Q. Tan, D.J. Clouthier, R.H. Judge, D.F. Plusquellic, J.L. Tomer and D.W. Pratt, J. Chem. Phys. 95 (1991) 7862.
[31] P. Groner and J.R. Durig, J. Chem. Phys. 66 (1977) 1855.
[32] P. Groner, J.F. Sullivan and J.R. Durig, in: Vibrational spectra and structure, Vol. 9, ed. J.R. Durig (Elsevier, Amsterdam, 1981).
[33] M. Noble and E.K.C. Lee, J. Chem. Phys. 81 (1984) 1632.